Wetting dynamics of thin liquid films and drops under Marangoni and centrifugal forces



2009 J. Phys.: Condens. Matter 21 464123

(http://iopscience.iop.org/0953-8984/21/46/464123)

IOP PUBLISHING JOURNAL OF PHYSICS: CONDENSED MATTER

J. Phys.: Condens. Matter **21** (2009) 464123 (9pp) doi:10.1088/0953-8984/21/46/464123

# Wetting dynamics of thin liquid films and drops under Marangoni and centrifugal forces

**Shomeek Mukhopadhyay and Robert P Behringer**

Department of Physics and Center for Nonlinear and Complex Systems, Duke University, Durham, NC 27708, USA

Received 12 May 2009, in final form 7 June 2009
Published 29 October 2009
Online at stacks.iop.org/JPhysCM/21/464123

**Abstract**

This paper presents an experimental study on thin liquid drops and films under the combined action of centrifugal forces due to rotation and radial Marangoni forces due to a corresponding temperature gradient. We shall examine thinning of a given liquid layer both with and without rotation and also consider the onset of the fingering instability in a completely wetting liquid drop. In many of the experiments described here, we use an interferometric technique which provides key information on height profiles. For thick rotating films in the absence of a temperature gradient, when an initially thick layer of fluid is spun to angular velocities where the classical Newtonian solution is negative, the fluid never dewets for the case of a completely wetting fluid, but leaves a microscopic uniform wet layer in the center. Similar experiments with a radially inward temperature gradient reveal the evolution of a radial height profile given by $h(r) = A(t)r^{\alpha}$, where $A(t)$ decays logarithmically with time, and $\alpha \simeq 0.8$. In the case where there is no rotation, small centrally placed drops show novel retraction behavior under a sufficiently strong temperature gradient. Using the same interferometric arrangement, we observed the onset of the fingering instability of small drops placed at the center of the rotating substrate in the absence of a temperature gradient. At the onset of the instability, the height profile for small drops is more complex than previously assumed.

(Some figures in this article are in colour only in the electronic version)

## 1. Introduction

In this paper, we present the results of an experimental study on thin films and drops under the action of centrifugal forces (due to rotation) and Marangoni forces or surface tension gradients (arising from a radial temperature gradient). To our knowledge, this is the first experimental study to combine a radial temperature gradient with centrifugal forces to study the dynamics of thin fluid films.

The study of rotating fluids has a long and illustrious history in fluid dynamics. At large Reynolds numbers, rotating fluids are of central importance in geophysical and oceanographic flows and at low Reynolds numbers they play an important part in industrial processes such as spin coating and locomotion in biological objects. In the industrial spin coating process, for example, it is undesirable to have any fingering instabilities or non-uniformities in the final layer. However, it is not just the Reynolds number which separates large scale geophysical flows from low Reynolds number 'thin film' flows. At low Reynolds numbers, wetting forces (through van der Waals forces and disjoining pressure) are dominant and the competition between wetting forces and externally applied forces can give rise to various instabilities. In particular, the three-phase contact line where the solid, liquid and vapor meet is still not completely understood and is an area of active research. In addition, an interesting question concerns the connection of the thin film solution to the large scale rotating flow when both types of behavior occur simultaneously.

### 1.1. Previous work

Regarding films, driven by rotation, one of the first analyses of isothermal spin coating was done by Emslie [1], who considered the evolution of a thin axisymmetric film of rotating fluid on a substrate rotating with a constant angular velocity. The exact solution of the problem, using only centrifugal and

 

viscous shear forces, showed that initially non-uniform profiles tend to become uniform. Surface tension and disjoining pressure were not included in the analysis.

The dynamics of thin films with both vertical heating and variable viscosity have been explored by many authors [2–4], while Stillwagon *et al* [5] have explored numerically and experimentally the effect of uneven substrates. In addition, applications to heat and mass transfer, specifically those related to spinning disk reactors, have been recently explored by Matar *et al* [6]. The problem of rotating thin films under the action of a vertical thermal gradient has been analyzed in the context of spin coating [7], where Schwartz *et al* used the lubrication approximation to analyze the flow of thin films that were exposed to air and lay on a spinning substrate. Most of the previous work [7–10] has focused on the stability of small drops placed at the center of rotation, and in particular on the fingering instability of the rotating drops, in the absence of temperature gradients. Wu [11] has analyzed numerically the problem of spin coating of nonvolatile thin liquid films on an axisymmetrically heated disk. In particular, he analyzed the effect of a sharp, i.e. step function change, in the radial temperature profile and predicted the existence of viscous shocks. These shocks have not yet been experimentally observed. In the problem analyzed by Wu [11], the temperature profile was hot at the center and cold on the outer rim. Hence the surface tension gradient aided the centrifugal force in draining the fluid film, and instabilities which might have arisen from opposing Marangoni and centrifugal forces were not considered.

Regarding drops on a rotating substrate, one of the earliest works to consider the fingering instability was performed by Melo *et al* [10], who stroboscopically followed the time evolution of milliliter sized drops of silicone oil, and observed the onset of the fingering instability. They found that the capillary ridge was no longer circular before the onset of the instability, and that some features of the instability (critical radius for onset and film thickness) could be explained by using the lubrication model in polar coordinates.

Fraysse and Homsy [8] performed detailed experimental measurements of the fingering instability on both Newtonian and non-Newtonian fluids and compared their results to a simple lubrication model. They found that the experimentally measured values for the azimuthal wavenumber and growth rate of the observed fingering were in agreement with the simple theoretical model, provided that the experimentally measured values of the critical radius of the drop at the onset of the instability were used. More recently, Schwartz and Roy [7] performed detailed numerical calculations for the spin coating problem in cylindrical coordinates within the framework of lubrication theory, paying particular attention to the contact angle. In both experiments and simulations it was assumed that the drop separates into a flat region and then forms a capillary ridge from which the fingers emerge.

In a previous study of wetting behavior of non-isothermal drops, Erhard and Davis [12] used a vertical temperature gradient. They reported either a speeding up or slowing down of the drop (depending on the direction of the temperature gradient), which was caused by the presence of macroscopic flows due to convection currents in the drop. Recently, there has been some interest in controlling drop movement by using chemical modification of surfaces. Also, Daniel *et al* [13] explored the condensing and merging of drops on a surface with a radial surface tension gradient.

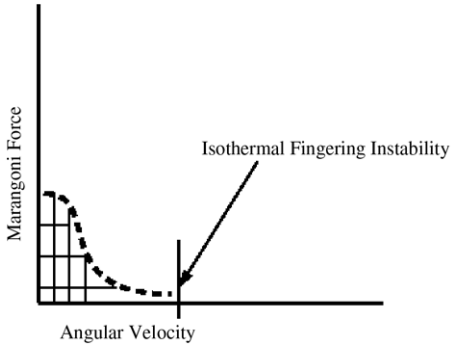


**Figure 1.** A schematic of the 'hypothetical' parameter space of thin film dynamics under the action of both Marangoni and centrifugal forces.

### *1.2. Parameter space, governing equations, and nondimensionalization*

In order to understand the various physical mechanisms involved, we consider a nominal parameter space as shown in figure 1. The $x$-axis, which corresponds to isothermal rotation, has been the most well studied part of the parameter space. The $y$-axis, which corresponds to the case of a drop or film moving or retracting under a radial temperature gradient, has been studied much less. The cross-hatched area under the dashed curve in the figure represents a region of interest, whose properties and transitions we map out in a preliminary fashion here. The Marangoni force is a surface force which arises when a fluid is subject to a temperature gradient. The surface tension of most Newtonian fluids decreases with temperature which creates a force from the hot to the cold side, when the fluid is placed in a temperature gradient.

In order to understand the time evolution of thin films in the context of rotating and radially heated flows, we consider the axisymmetric version of the lubrication equation which includes surface tension, Marangoni forcing, and disjoining pressure,

$$\frac{\partial h}{\partial t} + \frac{1}{r}\frac{\partial}{\partial r}\left\{\frac{\tau}{2\mu}rh^2 + \frac{\rho\omega^2}{3\mu}r^2h^3 - rh^3\frac{\partial P(h)}{\partial r} + \frac{\gamma}{3\mu}rh^3\frac{\partial K[h]}{\partial r}\right\} = 0. \tag{1}$$

Here, the pressure function, $P(h)$, includes gravity and disjoining pressure and is given by

$$P(h) = \frac{\rho g}{3\mu}h + \frac{1}{3\mu}\Pi(h) \tag{2}$$

and $K[h]$ is the linearized mean curvature ($K = \nabla^2 h$),

$$K[h] = \frac{1}{r}\frac{\partial}{\partial r}\left(r\frac{\partial h}{\partial r}\right). \tag{3}$$

In the case of a completely wetting fluid, we might model the disjoining pressure as $\Pi(h) = -Ah^{-3}$ with $A > 0$. Here, $\gamma$ is the surface tension, $\omega$ the angular velocity, $\rho$ the fluid density, $\mu$ the viscosity, $g$ the acceleration due to gravity, and $\tau$ the radial stress (due to a Marangoni effect from the temperature gradient). Typical radial velocities in these experiments are $\sim 10^{-3}$ cm s$^{-1}$, which implies that the Coriolis effect will be negligible compared to centrifugal effects and will not be considered.

In order to nondimensionalize the equation, we introduce a height scale, $H$, a radial scale, $R$ which is set by the radius of the container, or, in the case of a drop, by the initial drop radius, and a timescale, $T$, so that

$$h = H\tilde{h}, \qquad r = R\tilde{r}, \qquad t = T\tilde{t}. \tag{4}$$

The choice of $H$ and $T$ in each case is dictated by the particular experimental situation at hand. We then drop the tildes on all nondimensionalized variables, which gives the scaled equation in terms of nondimensional height $h$, radial length, $r$, and time, $t$, as,

$$\frac{\partial h}{\partial t} + \frac{1}{r}\frac{\partial}{\partial r}\left\{C_1 r h^2 + C_2 r^2 h^3 - C_3 r h^3 \frac{\partial h}{\partial r} - C_4 \frac{r}{h}\frac{\partial h}{\partial r} + C_5 r h^3 \frac{\partial K[h]}{\partial r}\right\} = 0, \tag{5}$$

where all the dimensional constants are combined in the following five nondimensional numbers,

$$C_1 = \frac{\tau H T}{2\mu R}, \qquad C_2 = \frac{\rho\omega^2 H^2 T}{3\mu}, \qquad C_3 = \frac{\rho g H^3 T}{3\mu R^2}, \qquad C_4 = \frac{AT}{\mu R^2 H}, \qquad C_5 = \frac{\gamma H^3 T}{3\mu R^4}. \tag{6}$$

In the following sections, we shall consider two main variations of the thin film problem. In one case, we observe the evolution of a single drop that is placed at the center of a rotating surface and is subject to both centrifugal and Marangoni forces. We also characterize the evolution of a thick (a few mm) fluid subject to thinning due to rotation and Marangoni forces.

## 2. Experimental apparatus

A schematic of the experimental apparatus is shown in figure 3. A key feature of the apparatus is that it allows the generation of radial temperature profiles. The basic apparatus consists of a rotating pre-wetted silicon wafer that rests on and is in good thermal contact with a cylindrical stainless steel base. The silicon wafer is 4 inches in diameter and has a highly polished oxidized surface. Rotation is provided by a stepper motor for precisely controlled rotation rates ($\omega/2\pi$) from ~10 mHz to ~10 Hz. An outer boundary restricts the fluid to a cylindrical region. The whole experiment sits on an optical table.

In order to create a radial temperature gradient, we pump cooling water from a recirculating cooler to the center of the substrate. The water returns through an annular channel. The outer rim is heated by a metal foil heater, attached to the copper ring. There are six embedded thermistors, which allow us to monitor the temperature radially along the substrate. We use slip rings to provide current for the heater and to monitor the thermistors. During a typical run, the cooler temperature and heater voltage are externally set and a subset of the thermistors is monitored constantly. All the thermistors are measured simultaneously at the beginning and the end of each run. A constant temperature gradient is generally established within 15–20 min of starting up, depending on the heater power used. The highest gradient that can be reached is about 20 K cm$^{-1}$ which is limited by the pumping capacity of the recirculating cooler and the heat exchanger, restricting the heater power to about 150 W. Figure 2 shows a typical temperature profile as recorded by the six thermistors embedded in the stainless steel base, just below the substrate. All distances are measured from the center of the cylinder.

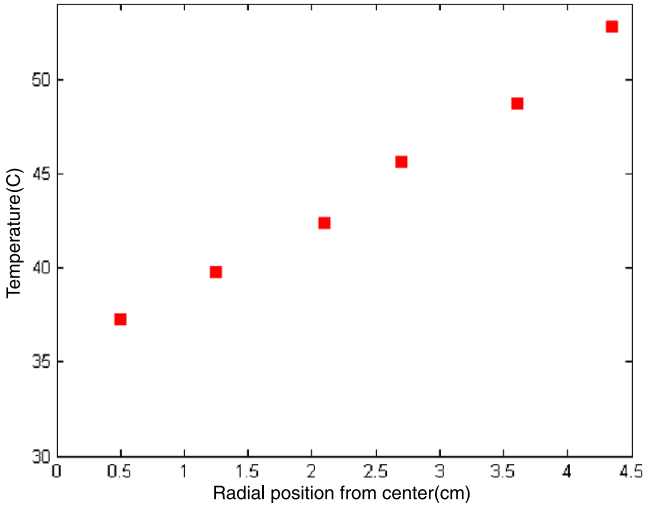


**Figure 2.** The radial temperature as recorded by the thermistors.

Imaging is carried out by illuminating the surface from above with either nearly monochromatic sodium vapor light (SVL), or with white light. The SVL source has two closely spaced lines at 587 and 591 nm. Generally, the average wavelength, i.e. 589 nm, is assumed. This provides an inexpensive way to illuminate a large diameter silicon wafer, and the low coherence of the sodium vapor lamp allows us to observe interference fringes without the extra speckle noise which arises in most He–Ne laser sources. When monochromatic light is incident on a thin fluid film, it is partially reflected by the top surface of the fluid and partially reflected by the highly polished silicon substrate on which it sits. These two reflected light beams generate an interference pattern where each fringe corresponds to a contour of constant height. For light of wavelength $\lambda$, traveling through a medium of refractive index $n$, the separation of the fringes is given by $\lambda/2n$, which is the minimum resolvable distance. With an SVL source and the fluids used here, the resolution is ~210 nm, which is slightly better than a He–Ne laser source ($\lambda = 632$ nm). In a typical thin oil film illuminated by white light, the fringes correspond to contours of equal chromatic order.

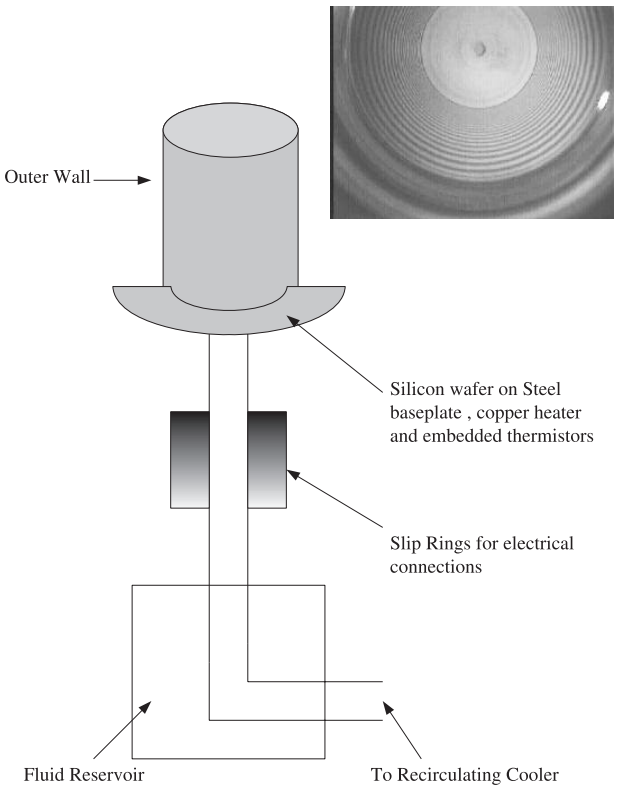


**Figure 3.** Schematic of the Marangoni spin coating apparatus. A circular resistive heater is attached to a copper strip at the outer rim of the stainless steel base. Six thermistors are embedded radially in the stainless steel base plate. The optical imaging system uses a beam splitter, sodium vapor light source, and a CCD camera placed above the rotating assembly. A typical interference image of the evolving thin film is shown in the inset.

For placing the drops as closely as possible to the geometrical center of the rotating surface, we use a specially machined device that fits snugly into the outer wall of the apparatus. A snug-fitting hole in the center of this piece guides a micro-pipette used to meter out drop volumes to a radial precision of 0.1 mm. For reference, the initial radius of the smallest drop used was around 0.5 mm. This centering plate is removed when imaging the fluid.

## 3. Experimental results

In the following subsections, we describe the results of three different experiments. In order, these are: (1) thinning of an originally thick film, (2) fingering instabilities of drops, and (3) advancing and retracting drops—a contrast of the effects of centrifugal and Marangoni driving. The forces that come into play include Marangoni, centrifugal, and disjoining forces. The disjoining force, which is positive for our experimental system (silicone oil on silicon wafer), causes the fluid to spread out on the substrate even in the absence of any externally applied force. In the case of thinning of a thick film, the Marangoni force opposes the centrifugal and disjoining forces. The fingering instabilities of small drops are caused by the interplay between centrifugal and disjoining forces and the instability is seen to happen above a certain critical rotational velocity. In the case of retracting drops the Marangoni force opposes the disjoining force and leads to an extremely slow thinning of the drop.

### *3.1. Thinning of a thick film*

The classical problem of a rotating cylinder of fluid with an open top and without any temperature gradient was first analyzed by Newton as an example of a non-inertial reference frame. In the absence of any surface tension and viscosity, the steady state free surface of the rotating fluid is given by

$$h(r) = H + (\omega^2/2g)(r^2 - R^2/2), \tag{7}$$

where $h(r)$ is the surface of the fluid at radial distance $r$, $H$ is the height of the fluid layer at rest, $R$ is the radius of the cylinder, $\omega$ is the angular velocity, and $g$ is the acceleration due to gravity. This solution neglects the damping effects of viscosity and curvature/wetting effects due to surface tension. If the angular velocity is increased beyond a critical value,

$$\omega_c = 2\sqrt{gH}/R, \tag{8}$$

then the above solution becomes negative for a range of $r$ near the origin. In fact, the classical solution is then piecewise continuous, with $h = 0$ below a critical radius and parabolic otherwise. The critical radius is given by

$$r_c = R\sqrt{(1 - \omega_c/\omega)} \qquad \omega > \omega_c. \tag{9}$$

One of the first and most interesting questions that one might ask is what role the wetting properties of the fluid have when the angular speed is increased above $\omega_c$. In fact, as we shall see later, for a partially wetting fluid, e.g. water on hydrophobic silicon, a hole opens up in the region where the classical solution is negative. However, for a completely wetting fluid, e.g. polydimethyl siloxane (PDMS) on a silicon wafer, the fluid in the central region reduces to a very thin film and never dewets even for the longest possible runs.

The dynamics of the thinning process can also be affected by applying a radial temperature gradient. If the temperature gradient is directed inward, then in the usual case, the outward centrifugal forces compete with the Marangoni forces which act radially inward.

We investigate the dynamics of the thinning process using the experimental apparatus as outlined in section 2. An example of the evolution of the fluid/film profile in the case of an isothermal thinning film is illustrated via the interference patterns shown in figure 4. We observe experimentally that if a completely wetting fluid is replaced by a partially wetting fluid like water or glycerol, then a bare spot is formed, along with a few droplets in the center. The formation of the bare spots and the asymptotic thinning of the thin films have been studied elsewhere [14, 15]. It is not surprising that a partially wetting fluid can undergo a 'bare spot' formation, since at high centrifugal forces, the surface tension disjoining pressure forces can be easily overcome.

We now consider the interference fringes of figure 4 and the inset in figure 3 in detail. One of the first things to notice is the flat region in the center. Since the color in white light is

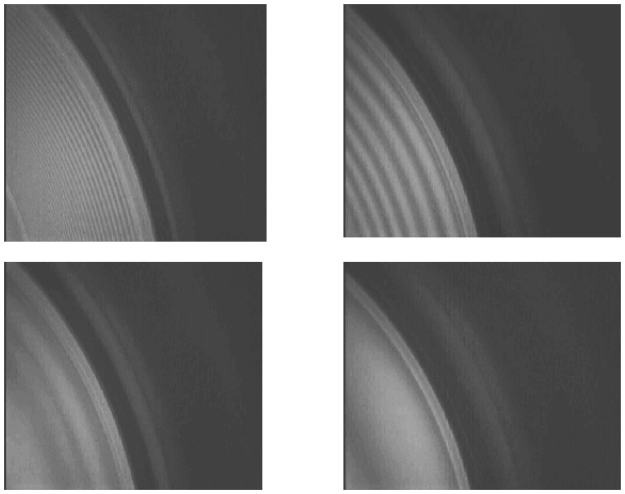

**Figure 4.** Closeup of the time evolution of interference fringes at 30 revolutions $s^{-1}$ for 50 centistokes PDMS oil shown 300 s apart, clockwise from top left. Illumination is by sodium vapor lamp. The images show a section where the thin film joins the classical Newtonian solution, seen here as the dark outer band without fringes. Note the thickness of the fringes increases with time as the inner layer thins.

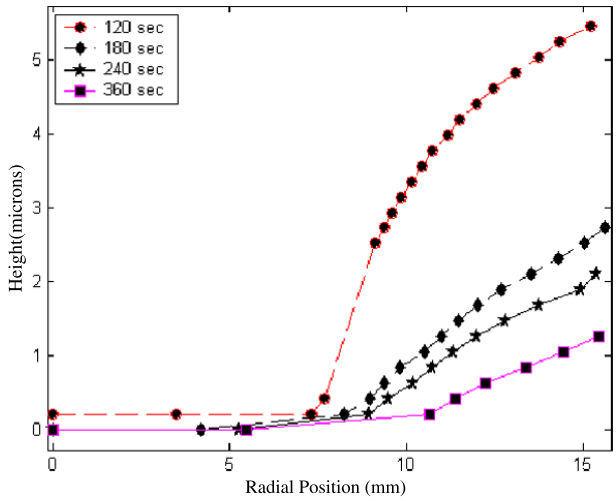


**Figure 5.** The evolution of the height profile for 50 centistokes PDMS rotating at 0.500 Hz shown for four different times. The film in the center decays rapidly to a greenish-blue hue after a few hundred seconds.

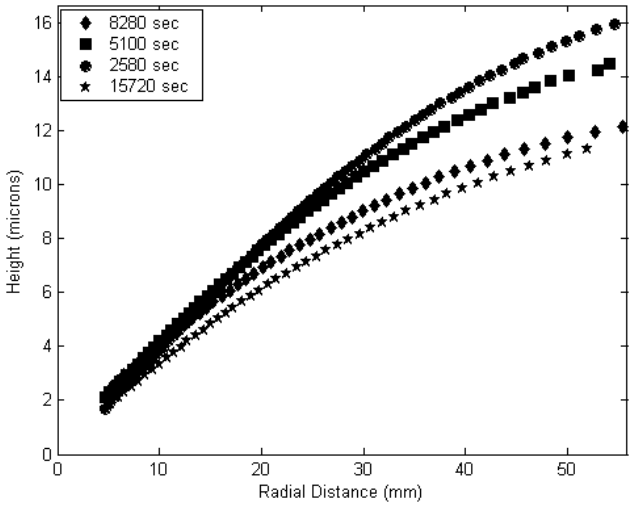


**Figure 6.** The evolution of the height profile for 10 000 centistokes PDMS rotating at 0.500 Hz and a temperature gradient of 8.1 K $cm^{-1}$. The inset shows the corresponding time for each profile.

uniform in this region, this implies that if there are any height changes they are definitely smaller than 200 nm. Following the initiation of rotation, this flat region slowly expands outward, with typical radial speeds of a few 'mm $min^{-1}$' and takes on a greenish-blue hue under white light. However, the center never dewets completely.

It is instructive to compare the fringes in this case to the ones in [16]. By counting the fringes, we can reconstruct a profile of the height. The separation between two dark or two bright fringes is 210 nm. Since fringes in monochromatic light give information about the magnitude of the gradient of height and not the absolute height, this means that a given fringe configuration can correspond to either an increasing or decreasing solution as a function of $r$. However, as the film evolves in time, the interference rings move radially outward, which is consistent with a monotonically increasing solution. From the detailed interference image, as shown in figure 4, we see that the width of the fringes beyond the central flat region increases in time, which indicates that the film is thinning. Hence, the slope of the layer decreases with time. This thin fluid layer connects the flat central region to the parabolic Newtonian solution on the outside. For isothermal thinning, examples of such profiles inferred from the interference fringes are given in figure 5.

The most interesting thing to note from the height profile is that the curvature is opposite (convex downwards) to that of the macroscopic Newtonian parabola (not shown, but convex upwards). The flat region in the center expands outward as time evolves. Note that in all the cases noted above the fluid is flowing under the combined effect of Marangoni and centrifugal forces which we follow experimentally by looking at the change in the free surface, i.e. height profile with time.

We next consider the effect of adding a temperature gradient, in addition to the wetting and centrifugal forces. We note that the disjoining pressure for a wetting fluid will actually act in concert with the Marangoni forces and help prevent dewetting. We start with a thick layer (a few mm) of PDMS on the silicon wafer once the temperature gradient has been established. From each run, the temperature gradient is calculated from the slope of the position versus temperature plot, e.g. figure 2. After the layer has been put on the wafer, it is generally spun at a high speed of around 5 Hz for half an hour. As discussed in the previous paragraph, this leaves a thin uniform layer at the center. After some time, the speed is lowered to 0.500 Hz, and the evolution of the thin film at the center is followed for several hours. The temperature gradient is kept constant during the whole cycle. Even for very long runs, lasting up to 30 h, the thin film at the center never reaches a flat, uniform profile, as was seen in the case

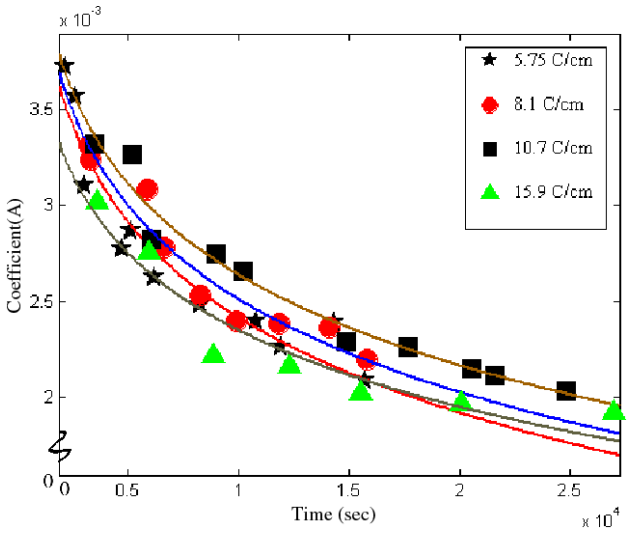


**Figure 7.** The evolution of the amplitude $A(t)$ as a function of time for four different temperature gradients assuming that $\alpha$ is fixed at 0.8. The curves show a logarithmic fit of the form $A = 1/(a + b\ln(t))$.

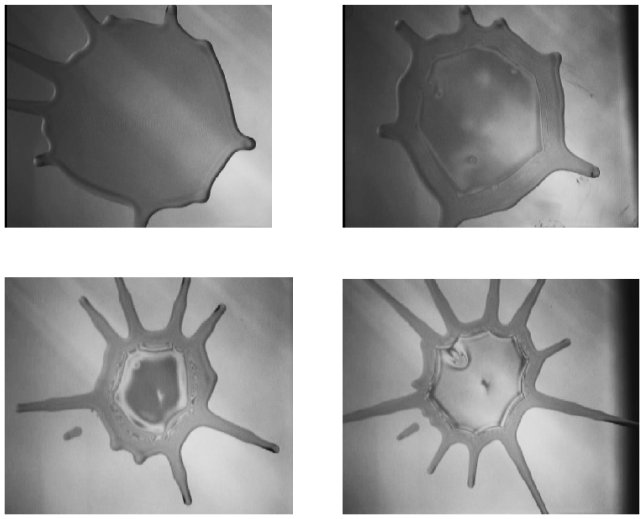

**Figure 8.** Evolution of fingers for drops of various volumes under a sodium vapor lamp. Top left shows a 10 ml drop where the flat region and the capillary ridge are observed. Top right shows a 5 ml drop where the flat region at the center evolves into the capillary ridge, and fringes are visible. The bottom two panels show a 100 $\mu$l drop shown at two different times separated by 500 s. Note the complicated fringe profile well after the onset of the fingering instability. All images are for 1000 centistokes PDMS and rotation rates of 5 Hz.

for isothermal rotation. Figure 6 shows experimental plots of the time evolution of the height profile for a temperature gradient of 8.1 K cm$^{-1}$. All the height profiles are obtained for $\omega/2\pi = 0.500$ Hz. Note that although the film profile thins out progressively in time, there is no 'flat region' at the center as in the case of isothermal rotation.

In this case, it is possible to fit power laws, $h(t) \sim A(t)r^{\alpha(t)}$ to the height profile as a function of time. Both $A(T)$ and $\alpha$ are, in principle, functions of time. However, to a very good approximation, we may treat $\alpha$ as a constant, $\alpha = 0.8$, and assume that all the time dependence is contained in $A(t)$. $A$ changes from 5, when the temperature gradient is 5.75 K cm$^{-1}$, to 0.2 when the temperature gradient is 15.9 K cm$^{-1}$. In figure 7, we see that the amplitude $A(t)$ decays logarithmically slowly, a particularly novel feature.

### *3.2. Fingering instabilities of drops*

In this section, we show experimental results for fingering instabilities of small drops where the temperature gradient has been turned off, so there is no Marangoni force. The results in this section are also distinguished by the fact that we use relatively small drops ranging in volume from about 100 $\mu$l to about 10 ml in volume. The initial radii of the drops range from ~5 mm for a 100 $\mu$l drop to ~2 cm for a 10 ml drop.

A particularly interesting observation from this study is that the onset of instability can be characterized initially by the formation of a single finger, which is followed at later times by other fingers. At the onset of instability we observe, as seen by previous workers, perturbations of the capillary ridge. However, below a certain characteristic viscosity-dependent rotation rate (for 1000 centistokes this corresponds to $\omega_{\text{critical}} = 1.5$ Hz), all the fingers do not nucleate at the same time, as is seen for example in [10].

As discussed above, it is generally assumed in analytical calculations and in numerical simulations that the only substantial curvature occurs around the outer rim/capillary ridge, and that the rest of the drop is a flat film, corresponding to two well separated height scales. In fact, extensive experimental observations show that the flat state in the center is only reached at large times or large drop volumes. To support these observations, we show in figure 8 fingering profiles for 500 centistokes silicone oil for long times where the asymptotic flat profile in the center is reached, and compare these with drops having a much smaller volume of 100 $\mu$l. In the top left panel, for a drop volume around 10 ml, the shape of the drop is similar to what has been previously observed. For small drop volumes, as for example in the second panel on the top right, this clean separation of lengths becomes 'blurred', and for volumes of 100 $\mu$l or less the film in the center is joined to the outer ridge by a complicated height profile, as seen from the interference fringes under SVL. For the smaller drops used here, no flat section in the center can be identified when the fingers emerge from the droplets. Hence, it is not possible to separate the flow at the onset into a ridge and flat section with two different height scales, as seen for example in the larger drops studied by Schwartz and Roy [7]. At the onset of the instability, when a single finger emerges, the height profile starting from the center to the capillary ridge has a parabolic profile, rather than a flat region connecting the capillary ridge to the center. For long times, however, separation of height scales, i.e. a flat central region and two strongly curved ridges on the outer periphery, occurs.

Some additional comments concerning the placement of the drops is of importance. As noted in the discussion of the experimental apparatus, a special insert is used for drop centering. However, it is possible that the rotational axis has a slight eccentricity with respect to the geometrical axis. The

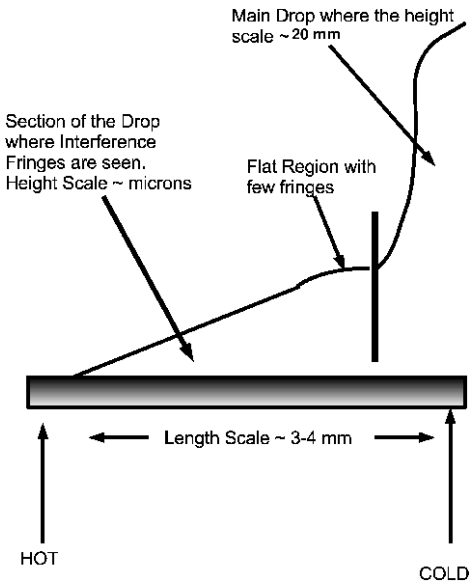


**Figure 9.** Schematic of a profile for a retracting drop. The vertical bar in the figure corresponds to the edge of the main drop. See figure 10 for the actual interferometric image. The center of the drop is about 2 cm from the retracting edge.

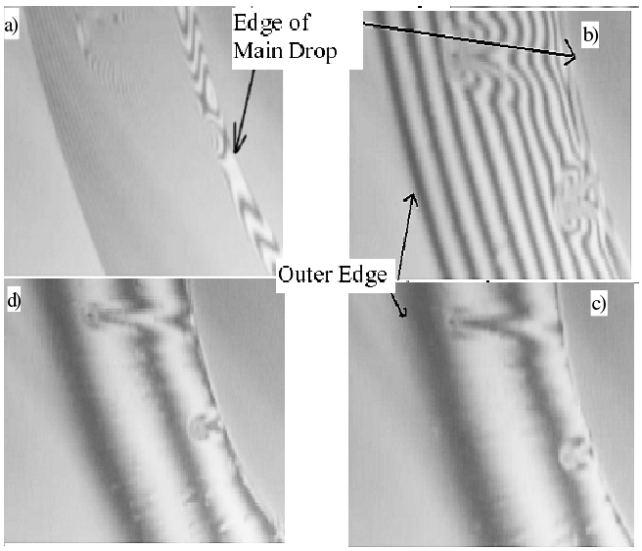


**Figure 10.** Closeup of the edge of the retracting drop for four different times. Clockwise from top left (a) 200 s, (b) 1000 s, (c) 3000 s, and (d) 20 000 s. The outer edge has moved inwards relative to the main drop. The field of view is 2.5 mm × 2.5 mm. Refer to the schematic in figure 9 for the profile. The initial drop radius, at the beginning of retraction was 1.2 cm and the temperature gradient was 12 K cm$^{-1}$.

importance of this eccentricity, if present, to the onset of the fingering instability, is not entirely clear at present.

### *3.3. Advancing and retracting drops*

In this section, we consider a perfectly wetting drop placed at the center of our apparatus and driven only by temperature gradient, i.e. the $\omega = 0$ limit of the parameter space. One of the most interesting experimental observations is that for large enough temperature gradients, a completely wetting fluid can be made to retract to a smaller equilibrium radius set by the gradient and droplet volume. For all the measurements described in this section, the drops have a volume of 10 $\mu$l s, which makes the gravitational force negligible.

Initially, a drop is placed at the center, where it spreads isothermally for a certain amount of time. After a modest amount of time, the radii for most drops are between 5 and 10 mm. We then switch on a temperature gradient. The spreading and the retraction take place on timescales which are much larger than the typical scales (∼10 min) required to change the temperature gradient. About ∼1000 s after the gradient is switched on, a flat region appears between the outer section of the drop and the central part. And overall, the drop takes about an hour or so to stop spreading. The drop then begins to retract. The major features of the retraction are shown in figure 9. As mentioned above, we observe a central portion of the circular drop, where the height scales are of the order of millimeters, that is joined by a flat section, which is equivalent to a meniscus, to the thin film on the outside. Note that most of the drop has withdrawn radially inward from the originally covered substrate, but a thin film remains because of the wetting nature of the fluid. Over a length scale of a few millimeters, the height changes from microns to the order of millimeters, although with an interference technique we can only probe the thin fluid film on the outside and not the thicker central part.

The interference images of the retracting drop are shown in figure 10, at four different times. In the beginning, the thin film on the outside is joined to the main drop by a flat section with very few fringes, as shown in panel (a). Around 1000 s, fringes appear and merge into the main drop, panel (b). As the drop retracts, the number of fringes decreases as shown in panels (c) and (d) of figure 10, indicating that the film is flattening out with time. The thin film withdraws at a very slow rate, and it also thins as it withdraws. The edge of the film undergoes increasing roughening with time as seen in the last two frames of figure 10.

The retraction of the outer edge is an increasingly slow process where velocities are typically of $\sim 10^{-5}$ mm s$^{-1}$. This is at least two orders of magnitude smaller than the spreading velocities of the same fluid (PDMS) under isothermal conditions. The capillary number, which is given by $\mu V/\gamma$, where $\mu$ is the viscosity, $\gamma$ is the surface tension, and $V$ is the velocity, is extremely small, since the retracting velocities are very small and both viscosity and surface tension are finite. Such vanishingly small capillary numbers give rise to interesting mathematical problems for the asymptotic analysis of the retracting drop dynamics.

As the film thins, the height of the thin film decreases. Equating the disjoining pressure term, $C_4$, with the Marangoni driving term, $C_1 = \tau HT/2\mu R$, we obtain a radial length scale $R = A/\tau H^2$, and a timescale $T = 2\mu A/\tau^2 H^3$. Using the standard value of $A = 1.4 \times 10^{-12}$ ergs for PDMS on oxidized silicon wafer gives a radial length scale of $\sim 7.5 \times 10^{-10}$ cm and a timescale of $\sim 3.8 \times 10^{-7}$ s. We contrast the ratio of these two scales with the typical observed radial velocities of

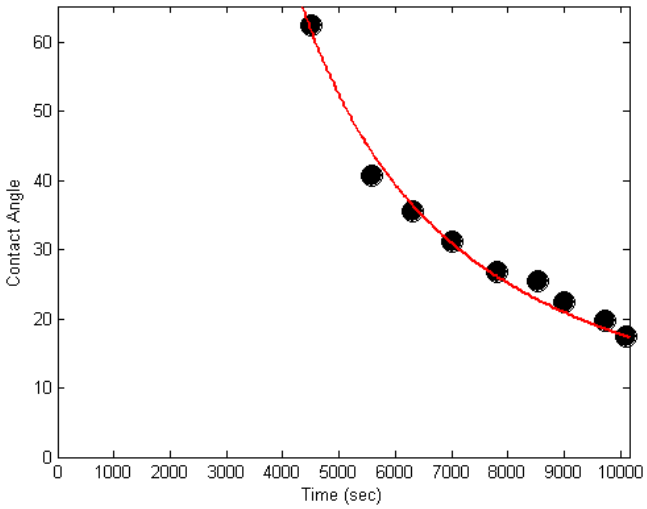


**Figure 11.** The time evolution of the estimated contact angle for the thinning drop. The line is a fit to $t^{-1.5}$.

the retracting drop of $\sim 10^{-5}$ mm s$^{-1}$. We note that the rate of change of the slope of the thin film, $\mathrm{d}\theta/\mathrm{d}t$, is generally $\sim 10^2$ faster than the retraction speed. This shows that the thinning out process from the outer edge to the main drop proceeds at a much faster speed than the speed at which the contact line is driven inwards by the Marangoni force.

In figure 11, we show the change of the contact angle with time, where the contact angle is extracted from the height profile by counting fringes as described in section 3.2. The curve is a least-squares fit to the data and has the form $\theta \sim t^{-1.5}$. By contrast, Tanner's law for spreading of the same wetting fluid is given by $\theta \sim t^{-0.3}$. This is a highly unusual exponent and it should be borne in mind that simple receding contact angle hysteresis cannot explain this since there is no advancing contact line in this system. The droplet recedes into the main body of the drop with time and for a perfectly wetting fluid, as in our experimental system, one does not expect any contact line hysteresis.

## 4. Conclusions and future work

In this paper, we describe experiments on rotating drops and thin films with and without the additional novel feature of a radial temperature gradient. To the best of our knowledge, this is the first experimental study of the evolution of a thin film under the effect of both centrifugal and radial Marangoni forces.

For thick rotating films in the absence of a temperature gradient, we explore the connection between a thinning centrifugally driven film and an outer solution having the 'Newton's bucket' form. We found that when an initially thick layer of fluid is spun at sufficiently high angular velocities, such that the classical Newtonian solution is negative, the fluid never dewets for the case of a completely wetting fluid. In the case of isothermal rotation, the final observed state was a central uniform thin film, which appeared greenish-blue in white light and exhibited no interference fringes in monochromatic or white light. This forms the backdrop for similar experiments with the addition of a radially inward temperature gradient. The evolution of the height profile when a radial temperature gradient was applied to the rotating thin film was studied in detail and we obtained an empirical scaling for the profiles. Specifically, we found a universal radial dependence of the height given by $h(r) = A(t)r^{\alpha}$, where $A(t)$ decays logarithmically with time, and where $\alpha \simeq 0.8$ appears constant.

We then explored the behavior of small drops in the absence and presence of radially inward temperature gradients. In the case where there is no rotation but only a temperature gradient, we observed that it is possible to make a completely wetting drop retract under the application of a sufficiently strong temperature gradient. Using the same interferometric arrangement, we observed the onset of the fingering instability of small drops placed at the center. At the onset of the instability, the height profile is far more complex than what is observed for larger drops. A clean separation into a flat part and a separate capillary ridge turns out to be the exception rather than the rule in our studies. We note that the use of an interferometric technique provides new information that was not available in previous work [10] based on shadowgraph or stroboscopic techniques. The interferometric approach demonstrates that at the onset of the instability for small drops there is a complex height profile. We note, too, that in the present experiments, we observe cases where the initial instability can start from a single finger before forming up to as many as 12, in contrast to the experiments of Melo *et al* [10] for which the instability typically starts from four fingers.

Currently, modeling and numerical studies are being undertaken to gain insight into the rich phenomenology observed in this experimental system. Future work will involve looking at the effect of Marangoni forces on the fingering instabilities of rotating drops. Other exciting possibilities involve probing the behavior of complex fluids, such as non-Newtonian fluids or liquid crystals.

## Acknowledgments

We would like to thank Tom Witelski, Mike Gratton, Rich Mclaughlin, Michaela Froelich, and Bjorn Samuelsson for extensive discussions and Richard Nappi for help in the machine shop. This work was supported by the National Science Foundation under grant number DMS-02444498.

## References

[1] Emslie A G, Bonner F T and Peck L G 1958 Flow of a viscous liquid on a rotating disk *J. Appl. Phys.* **29** 858
[2] Kitamura A 2001 Thermal effects of liquid film flow during spin coating *Phys. Fluids* **13** 2788
[3] Usha R, Ravindran R and Uma B 2005 Dynamics and stability of a thin liquid film on a heated rotating disk with variable viscosity *Phys. Fluids* **17** 102103
[4] Mckinley I S, Wilson S K and Duffy B R 1999 Spin coating and air-jet blowing of thin viscous drops *Phys. Fluids* **11** 30
[5] Stillwagon L E and Larson R G 1990 Leveling of thin films over uneven substrates during spin coating *Phys. Fluids* A **2** 1937

[6] Matar O K, Lawrence C J and Sisoev G M 2005 The flow of thin liquid films over spinning disks: hydrodynamics and mass transfer *Phys. Fluids* **17** 052102
[7] Schwartz L W and Roy R V 2004 Theoretical and numerical results for spin coating of viscous liquids *Phys. Fluids* **16** 569
[8] Fraysse N and Homsy G M 1994 An experimental study of rivulet instabilities in centrifugal spin coating of viscous newtonian and non-newtonian fluids *Phys. Fluids* **6** 1491
[9] Spaid M A and Homsy G M 1997 Stability of viscoelastic dynamic contact lines: an experimental study *Phys. Fluids* **9** 823
[10] Melo F, Joanny J F and Fauve S 1989 Fingering instability of spinning drops *Phys. Rev. Lett.* **63** 1958
[11] Wu L 2006 Spin coating of thin films on an axisymmetrically heated disk *Phys. Fluids* **18** 063602
[12] Erhard E and Davis S H 1974 Non-isothermal spreading of liquid drops on horizontal plates *J. Fluid Mech.* **229** 365
[13] Daniel S *et al* 2001 Fast drop movement resulting from the phase change on a gradient surface *Science* **291** 633
[14] Dandapat B S, Daripa P and Ray P C 2003 Asymptotic study of film thinning process on a spinning annular disk *J. Appl. Phys.* **94** 4144
[15] Ungarish M and Mang J 2003 The flow field and bare-spot formation in spin-up from rest of a two layer fluid about a vertical axis *J. Fluid. Mech.* **474** 117
[16] Alles H, Ruutu J P, Babkin A V, Hakonen P J, Lounasma O V and Sonin E B 1995 Observations on superfluid meniscus in rotating $he^3 - b$ *Phys. Rev. Lett.* **74** 2744